THE JOURNAL OF BIOLOGICAL CHEMISTRY VOL. 280, NO. 45, pp. 37846–37852, November 11, 2005

Differential Requirement for Phospholipase D/*Spo14* and Its Novel Interactor *Sma1* for Regulation of Exocytotic Vesicle Fusion in Yeast Meiosis*

Received for publication, April 19, 2005, and in revised form, August 8, 2005 Published, JBC Papers in Press, September 7, 2005, DOI 10.1074/jbc.M504244200

Christian G. Riedel[1,2], **Massimiliano Mazza**[1], **Peter Maier, Roman Körner**[3], **and Michael Knop**[4]

From the Cell Biology and Biophysics Unit, European Molecular Biology Laboratory, D-69117 Heidelberg, Germany

During sporulation and meiosis of budding yeast a developmental program determines the formation of the new plasma membranes of the spores. This process of prospore membrane (PSM) formation leads to the formation of meiotic daughter cells, the spores, within the lumen of the mother cell. It is initiated at the spindle pole bodies during meiosis II. Spore formation, but not meiotic cell cycle progression, requires the function of phospholipase D (PLD/Spo14). Here we show that PLD/Spo14 forms a complex with Sma1, a meiotically expressed protein essential for spore formation. Detailed analysis revealed that both proteins are required for early steps of prospore membrane assembly but with distinct defects in the respective mutants. In the Δ*spo14* mutant the initiation of PSM formation is blocked and aggregated vesicles of homogenous size are detected at the spindle pole bodies. In contrast, initiation of PSM formation does occur in the Δ*sma1* mutant, but the enlargement of the membrane is impaired. During PSM growth both Spo14 and Sma1 localize to the membrane, and localization of Spo14 is independent of Sma1. Biochemical analysis revealed that Sma1 is not necessary for PLD activity *per se* and that PLD present in a complex with Sma1 is highly active. Together, our results suggest that yeast PLD is involved in two distinct but essential steps during the regulated vesicle fusion necessary for the assembly of the membranous encapsulations of the spores.

During cellular differentiation and development, tightly controlled cell polarity changes occur (1). These changes involve redirection of the secretory pathway and specify the site of exocytosis. For these processes, molecular mechanisms exist that ensure correct delivery of membranes and secretory proteins in response to cellular signals. During yeast gametogenesis (sporulation) so-called prospore membranes (PSMs)[5] form *de novo* at sites adjacent to the spindle pole bodies (SPBs), the centrosomes of yeast (2). This process involves redirection of the secretory machinery to the SPB (3) and results in formation of four haploid cells within the mother cell. The initiation of this process is a tightly regulated event that occurs exactly once per SPB at the onset of meiosis II. It is thought that PSM formation is initiated by the fusion of vesicles at the SPB that generate an initial compartment, which then subsequently becomes enlarged and grows around the haploid nucleus to which it is connected via the SPB. Only recently support for this model came from the analysis of a Δ*mso1* mutant in which a block of PSM formation on the level of vesicle fusion at the SPB was visible (39).

The formation of PSMs appears to require several genes known to act in the exocytosis of post-Golgi vesicles in vegetatively growing (mitotic) cells. In temperature-sensitive mutants of *sec1*, *sec4*, and *sec8* or cells deleted for the syntaxin *SSO1*, no PSM formation occurs at the restrictive temperature (3, 4). In addition, PSM formation requires Spo20, a sporulation-specific Sec9 target SNARE homologue (3). In Δ*spo20* cells the PSMs form but fail to capture the nuclei. This suggests that PSM biogenesis is a developmentally regulated branch of the exocytic pathway (3). Currently, the precise vesicle fusion machinery required for the initiation of membrane formation and the way that this machinery is regulated and how it correlates to the machinery required for subsequent membrane elongation during PSM growth are not known. One possible regulator of this pathway is phospholipase D (PLD/Spo14). Spo14 is only essential for spore formation and localizes to the PSMs (5). In mammalian cells, PLD has been proposed to participate in cytoskeletal modeling and vesicular traffic in the secretory pathway (6–8). This regulation is thought to occur mainly through its capacity to hydrolyze phospholipids in order to generate the second messenger phosphatidic acid (PA). Both the *Saccharomyces cerevisiae* PLD/Spo14 and the mammalian phospholipase D associate with phosphatidyl inositol-4,5-bisphosphate (PtdIns-4,5-P_2), and PtdIns-4,5-P_2 has been shown to be needed for efficient PLD function (9, 10) and for the localization of the mammalian PLD (11).

Previously, a systematic approach has identified several genes necessary for meiosis and sporulation (12). One of these genes, *SMA1*, showed a specific defect associated with the formation of the prospore membranes. Here we show that Sma1 is associated with Spo14, the phospholipase D of yeast, and that both proteins are required for related but distinct functions during the assembly of the prospore membranes. Our data are consistent with the idea that PLD plays several roles during this process, including one early Sma1-independent function during the initiation of membrane formation via homotypic vesicle fusion and a later function during elongation of the membrane by heterotypic membrane fusion in association with Sma1.

MATERIALS AND METHODS

Yeast Strains, Growth Conditions, and Plasmids—The yeast strains and plasmids used in this study are listed in TABLE ONE. For vegetative growth, standard conditions were used (13). For sporulation, the previously described pre-growth regime was used (14). Sporulation medium was 0.3% (w/v) potassium acetate in water. For cell biological and bio-

* This work was financially supported in part by the European Molecular Biology Laboratory and by Deutsche Forschungsgemeinschaft Grant KN498/2-2. The costs of publication of this article were defrayed in part by the payment of page charges. This article must therefore be hereby marked "*advertisement*" in accordance with 18 U.S.C. Section 1734 solely to indicate this fact.

[1] These authors contributed equally to this work.
[2] Present address: Institute of Molecular Pathology, Dr. Bohrgasse 7, A-1030 Vienna, Austria.
[3] Present Address: Max-Planck-Institut für Biochemie, Am Klopferspitz 18A, D-82152 Martinsried, Germany.
[4] To whom correspondence should be addressed. Tel.: 49-6221-387631; Fax: 49-6221-387512; E-mail: knop@embl.de.

[5] The abbreviations used are: PSM, prospore membrane; GFP, green fluorescent protein; HA, hemagglutinin; MALDI-TOF, matrix-assisted laser desorption ionization time-of-flight; MOPS, 4-morpholinepropanesulfonic acid; PA, phosphatidic acid; PC, phosphatidylcholine; PLD, phospholipase D; SNARE, soluble *N*-ethylmaleimide-sensitive factor attachment protein receptors; SPB, spindle pole body.

TABLE ONE

Yeast strains and plasmids

Strain	Genotype	Source
NKY289	*Mata ura3 lys2 ho*::*hisG* (SK-1 background)	37
NKY292	*Matα ura3 lys2 leu2*::*hisG ho*::*LYS2* (SK-1 background)	37
YKS32	Diploid obtained by crossing NKY289 and NKY292	14
LH175	*Mat a ho*:*hisG lys2 ura3 leu2 his3 trp1ΔFA* (SK-1 background)	Linda S. Huang/Ira Herskowitz
LH176	*Matα ho*:*hisG lys2 ura3 leu2 his3 trp1ΔFA* (SK-1 background)	Linda S. Huang/Ira Herskowitz
LH177	Diploid obtained by crossing LH175 and LH176	Linda S. Huang/Ira Herskowitz
YMK691	NKY289/292 with Δ*spo14*::*kanMX4*/Δ*spo14*::*kanMX4*	This study
YMK693	NKY289/292 with *natNT2-pCUP1-GFP-SPO14*/Δ*spo14*::*kanMX4*	This study
YMK695	NKY289/292 with *natNT2-pCUP1–3HA-SPO14*/Δ*spo14*::*kanMX4*	This study
YMK713-2	NKY289/292 with Δ*sma1*::*kanMX4*/Δ*sma1*::*kanMX4 natNT2-pCUP1–3HA-SPO14/natNT2-pCUP1–3HA-SPO14*	This study
YMM199-1	NKY289/292 with *SMA1-GFP-hphNT1*/*SMA1-GFP-hphNT1* Δ*spo14*::*kanMX4*/*natNT2-CUP1–3HA-SPO14*	This study
ESM356-1	*MATa ura3–53 leu2Δ1 his3Δ200 trp1Δ63* (S288c background)	This study
YAM255	LH175/LH176 with *SMA1–3HA-hphNT1/SMA1–3HA-hphNT1*	This study
YAM282-2	ESM356–1 containing *natNT2-pCUP1-eGFP-SPO14*	This study
YAM283-2	ESM356–1 containing *natNT2-pCUP1–3HA-SPO14*	This study
YAM307-1	YAM283–2 containing pCR3	This study
YKS53	*Mat**a**/α DON1-eGFP-kanMX4/DON1-eGFP-kanMX4*	14
YKS65-1	*Mat**a**/α* Δ*mpc70*::*kanMX4*/Δ*mpc70*::*kanMX4* Δ*mpc54*::*kanMX4*/Δ*mpc54*::*kanMX4 DON1-eGFP-kanMX4/DON1-eGFP-kanMX4*	14
YKS233	*Mat**a**/α SMA1-eGFP-kanMX4/SMA1-eGFP-kanMX4*	This study
YCR10	LH175/LH176 with *DON1-GFP-kanMX4/DON1-GFP-kanMX4* Δ*sma1*::*hphNT1*/Δ*sma1*::*hphNT1*	This study
YCR11	LH175/LH176 with *SMA1-ProtA-kanMX4/SMA1-ProtA-kanMX4*	This study
Plasmids	**Description**	**Source**
p423-ADH1	2-μm yeast plasmid containing the *HIS3* marker, the *ADH1* promoter and the *CYC1* terminator	38
pCR3	p423-ADH1-*SMA1* (SMA1 ORF cloned via Xho1 and Spe1)	This study
pET28c(+)	Bacterial expression plasmid (kan^R, T7, 6HIS)	Novagen
pMAX3-1	pET28c(+) containing full-length *SMA1* in Nco1/Xho1	This study
pUK22	pET28c(+) containing codon 1–200 of *SPO14* in BamH1/Xho1	This study

chemical analysis, sporulation was carried out until maximal amounts of cells (~60%) were undergoing meiosis II (5.5–6.5 h after induction of sporulation as judged by 4,6′-diamidino-2-phenylindole staining or Don1-GFP fluorescence, a marker of the developing PSM) (14). Gene deletion (of *SPO14* or *SMA1*) and C-terminal tagging of *SMA1* were performed using the previously described PCR strategy (15). N-terminal tagging of *SPO14* with either GFP or 3×HA (*GFP-SPO14* and *HA-SPO14*) was performed using a PCR-based insertion of the *CUP1-1* promoter (bp −472 to −1 of the promoter from the *CUP1-1* gene) using the previously described PCR tagging strategy (16). *SPO14* expression from the *CUP1* promoter was induced with 3 μM $CuSO_4$ at a time point during sporulation before the cells enter meiosis II (4 h after induction of sporulation). This leads to a wild type level of sporulation of the strains and a protein level of Spo14 that is ~2 to 3-fold higher than in wild type cells as judged using Western blotting and antibodies specific to Spo14. The plasmids used are shown in TABLE ONE. For cloning, routine molecular biological methods were used. PCR-cloned DNA fragments were fully sequenced.

Immunological Techniques and Antibodies—Purification of Sma1 tagged with protein A was performed using liquid nitrogen-mortared cells dissolved in buffer (10 mM triethanolamine, 150 mM NaCl, 5 mM EGTA, 5 mM EDTA, pH 7.5, and 1% Nonidet P-40) containing protease inhibitors (17) and nonspecific rabbit IgGs cross-linked to Dynabeads (Dynal). Upon several washes with the same buffer the proteins were eluted with 1% SDS at 65 °C for 5 min. Eluted proteins were analyzed using NU-PAGE 4–20% gradient gels (Invitrogen) with MOPS gel running buffer followed by Coomassie staining. Sma1-protein A was identified using the PAP detection reagent (Dako). Polyclonal antibodies specific for full-length Sma1 or Spo14 (amino acids 1–200) were generated using N-terminally His-tagged bacterial expressed proteins (plasmids pMAX3–1 and pUK22, respectively). Antibodies were affinity-purified. The specificity of the purified antibodies was verified using extracts of vegetative cells that either overexpress the protein (Sma1) or meiotic extracts of cells deleted for the *SPO14* gene (data not shown). Antibodies specific for tubulin, GFP, and Ady3 have been described previously (17). The HA (12CA5) used for immunoprecipitations was purchased from Roche Applied Science. Anti-HA immunoprecipitations of 3×HA-tagged proteins were performed using the same buffer as for protein A purification, and anti-HA (12CA5) monoclonal antibodies were cross-linked to protein G-Dynabeads (Dynal) according to the instruction of the manufacturer. Cells were broken using acid-washed glass beads and 50 OD_{600} units of cells in buffer without Nonidet P-40. Upon lysis Nonidet P-40 was added, and extracts were cleared at 10,000 rpm for 10 min. Upon immunoprecipitation the beads were

washed 5 times, and bound proteins were eluted with 6 M urea, 5% SDS, and 200 mM $Na_xH_yPO_4$, pH 6.8, at 65 °C for 5 min and adjusted to 100 mM dithiothreitol for gel electrophoresis. For immunofluorescence microscopy, cells were fixed with 3.7% formaldehyde for 60 min in the medium (adjusted to 0.1 M K_xH_yPO4, pH 6.5). Digestion of cells using Zymolyase 100T and immunolabeling was performed as described (14) (a detailed protocol can be obtained upon request). For double labeling (Figs. 2. *a–d*, and 3, *c* and *d*) primary antibodies (from mouse and rabbit) were detected using Cy2- and Cy3-labeled goat antibodies. For triple labeling, primary antibodies (from sheep, mouse, and rabbit) were detected using Cy2-, Cy3-, and Cy5-labeled donkey antibodies. In some cases, Alexa 486 was used as dye instead of Cy2. Faithful discrimination of different fluorophores was always verified using appropriate controls. For detection, filter sets from Chroma were used (Piston filter set for Cy2 and Alexa 486 and Cy3 and Cy5 filter sets). Images were recorded on a Leica DMX using a 100× PlanApo oil objective with a numerical aperture of 1.4 and a CoolSNAP cf camera (12 bit, 4.65 × 4.65 μm pixel size, 1392 × 1040 pixels) from Photometrics and Metamorph software. Image stacks were collected (0.3-μm spacing). Maximum projections containing the relevant slices (usually 4–5) are shown. Image processing was restricted to linear contrast enhancements. Electron microscopy of sporulating yeast cells using the glutaraldehyde/$KMnO_4$ protocol followed by Agar 100 embedding was performed as described previously (17).

Other Methods—Proteins were identified by tryptic peptide mass fingerprinting using matrix-assisted laser desorption ionization time-of-flight (MALDI-TOF) Reflex III instrument (Bruker Daltonik, Bremen, Germany) in positive ion reflector mode and probability-based data base searching. PLD activity assays, either using whole cells or immunoisolated protein complexes from sporulating yeast, were performed as described (5).

RESULTS

Mutants deleted for the *SMA1* gene are unable to form spores upon meiosis (12). To gain insight into the molecular function of Sma1, we tagged it with protein A and purified it from meiotic cell extracts. The Sma1-protein A fusion was fully functional as judged by its ability to promote spore formation (data not shown). This approach revealed one major co-purifying protein of ~200 kDa (Fig. 1*a*), which was subsequently identified using MALDI-TOF measurements as PLD/Spo14. The other co-purifying proteins were found to be most likely nonspecifically bound proteins (see "Discussion"). Co-immunoprecipitation experiments with extracts prepared from meiotic cells confirmed the interaction between Sma1 and PLD/Spo14 in both directions (Fig. 1*b*). In vegetative cells Sma1 is not expressed (data not shown) (18); however, when ectopically expressed, it co-immunoprecipitated with Spo14 (Fig. 1*c*). This result indicates that no meiosis-specific factor is required for the association of Sma1 with PLD/Spo14.

PLD/Spo14 was shown previously to be necessary for sporulation, and the protein, when over expressed, localized to the areas of the SPBs in meiosis II (5), the sites where the prospore membranes become assembled. Mutant cells deleted for *SPO14* are not affected in progression through meiosis but do not form spores, and the absence of immature spores was confirmed by electron microscopy (5). To characterize the meiotic Δ*spo14* phenotype with respect to prospore membrane assembly and compare it with the Δ*sma1* phenotype, we performed a detailed comparative characterization of Δ*sma1* and Δ*spo14* mutants during meiosis. For this, we first used fluorescence microscopy and antibodies specific for Ady3p, a marker for developing PSMs (Fig. 2*a*) (17). Tubulin staining was used to precisely identify cells in meiosis II

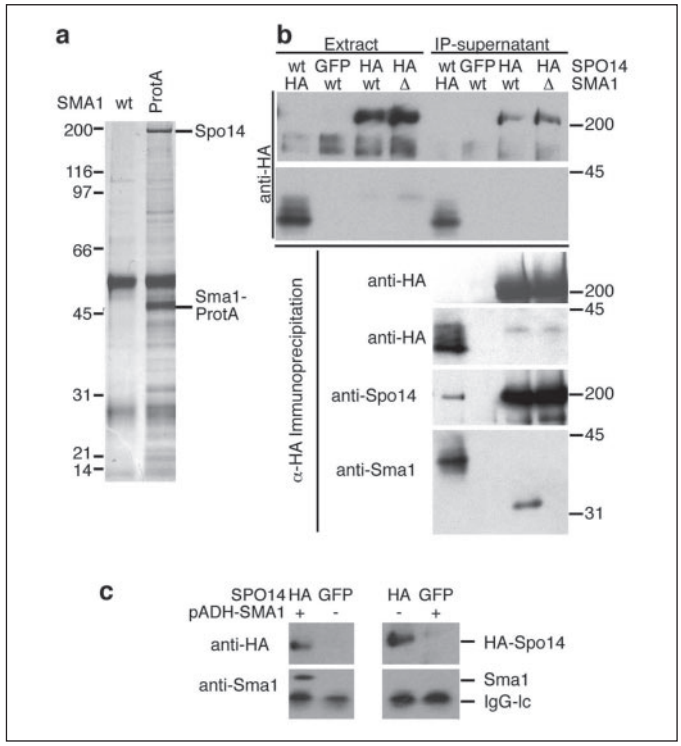

FIGURE 1. **PLD/Spo14 forms a protein complex with Sma1.** *a*, extracts from meiotic cells expressing Sma1-protein A (YCR11) or untagged Sma1 were used to immunoisolate Sma1-protein A/LH177 (*Sma1-ProtA*). Immunocomplexes were separated on 4–12% NuPage gels (Invitrogen) and Coomassie stained. *wt*, wild type. *b*, anti-HA immunoprecipitation (*IP*) of Sma1 with HA-Spo14 and Spo14 with Sma1-HA from meiotic cells. Meiotic extracts of the strains expressing the indicated constructs were used (*wt*, untagged; *GFP*, GFP-Spo14; *HA*, HA-Spo14 or Sma1-HA as indicated; Δ, chromosomally deleted for *SMA1*). Strains used were YMK693, YMK695, YAM255, and YMK713; all HA tags used were triple tags. The top two blots show HA-Spo14 and Sma1-HA present in the extracts before and after immunoprecipitations. The lower blots show detection of the indicated proteins in the immunoprecipitates using the indicated antibodies (two anti-HA blots and respective anti-Spo14 and anti-Sma1 blots). *c*, co-immunoprecipitation of Sma1 with HA-Spo14 from vegetatively growing (mitotic) cells. The presence of HA- and GFP-Spo14 (under *pCUP1-1* control) and a plasmid expressing *SMA1* under the control of the constitutive *ADH1* promoter in the cells as indicated. Strains used were YAM282 and YAM283. Plasmids used were p423-ADH and pCR3.

(two spindles within one cell) and the positions of the SPBs, which are at the ends of the microtubule bundles.

The results demonstrate that the Δ*spo14* mutant (Fig. 2*c*) and the Δ*sma1* mutant (Fig. 2*d*) fail to assemble prospore membranes. The Ady3 staining seen in the two mutants differs from each other, suggesting different defects with regard to prospore membrane assembly in the two mutants.

PSM assembly is initiated on top of the SPBs metaphase/anaphase of meiosis II (14, 19–21). For a more precise estimation of the defects, we also used a wild type strain and a strain deleted for two structural proteins of the meiotic SPB, Mpc54p and Mpc70p. In the wild type strain during the anaphase of meiosis II, Ady3 forms doughnut-shaped, ring-like structures in wild type cells (often visible as rods when viewed from top; see *white outlined arrowhead* in Fig. 2*a*), which are indicative of assembled PSMs. At this stage, Ady3 localizes to a coat governing the leading edge of the growing prospore membrane (LEP (leading edge protein) coat) (17). In the Δ*mpc54* Δ*mpc70* mutant the formation of the meiosis II-specific appendix of the SPB, the meiotic plaque, is impaired, and the assembly of PSMs is completely blocked (14, 22). In this case, Ady3 exhibited staining at the SPBs and dotted structures in the cytoplasm as shown previously (17) (Fig. 2*b*). Some of these dotted structures (called precursor structures) co-localize with the syntaxins Sso1 and Sso2 and may result from the clustering of secretory vesicles (17).

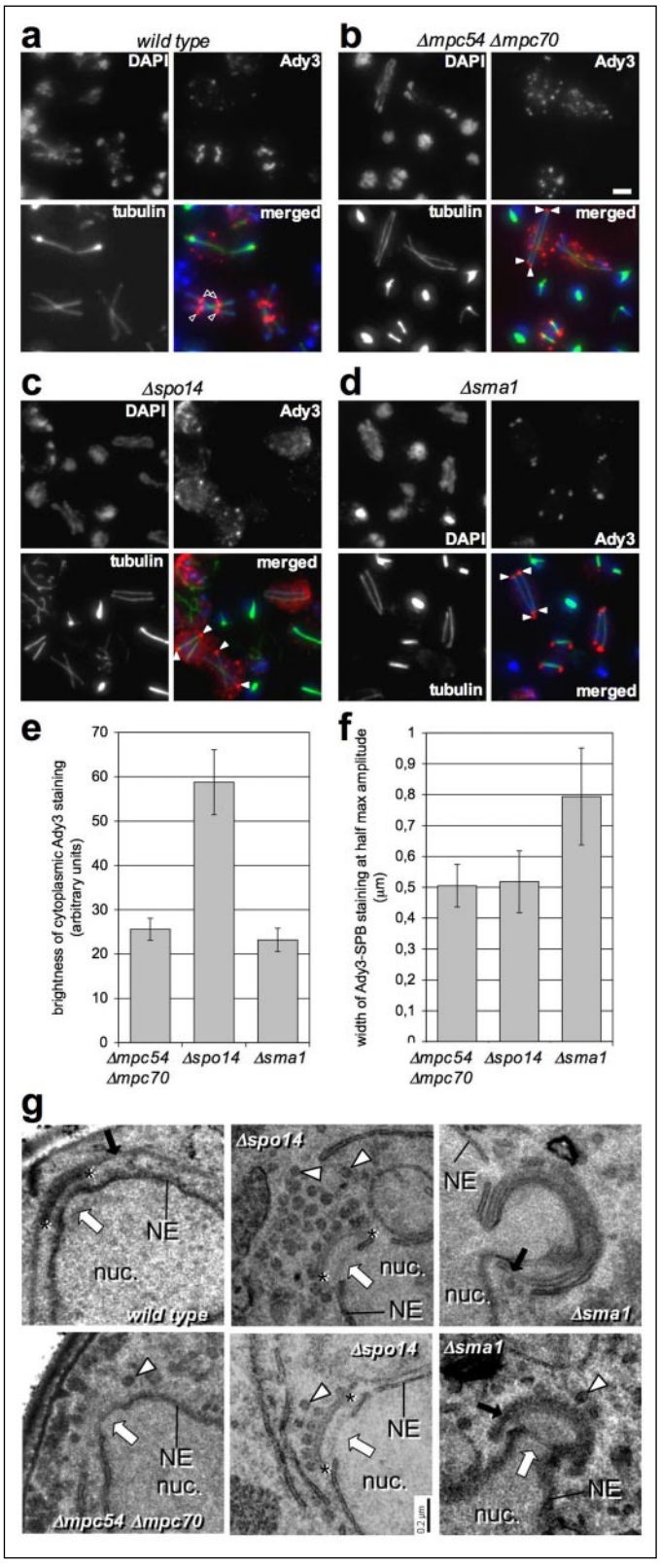

FIGURE 2. **Initiation of PSM membrane biogenesis at the SPBs is blocked at different steps in Δ*spo14*, and Δ*sma1* mutant cells.** *a–d*, strains studied were wild type (YKS53) (*a*), Δ*mpc54* Δ*mpc70* (YKS65) (*b*), Δ*spo14* (YMK691) (*c*), and Δ*sma1* (YCR10) (*d*). Populations of cells undergoing synchronous sporulation were used for this experiment. Cells were harvested at a time point with a high content of cells in meiosis II (after 6 h of induction of sporulation). Wide field immunofluorescence pictures of representative situations are shown. 4,6′-Diamidino-2-phenylindole (*DAPI*) staining of DNA, Ady3, and tubulin, as well as merged pictures, are shown. DNA and tubulin staining are indicative of the cell cycle stage of a cell. Cells in meiosis II are characterized by two bundles of microtubules. Ady3 detects a component of the LEP coat. In cells in meiosis I, Ady3 localizes to discrete dots in the cytoplasm and at the SPBs (next to the ends of microtubule bundles). In meiosis II, Ady3 localizes to a coat governing the opening of the prospore membrane (indicated by *outlined arrowheads* in *panel a*). In the mutants (*b–d*) some Ady3 localizes to the SPBs (indicated by *white arrowheads*). *Scale bar* for *panels a–d* (*in panel b*), 2 μm. *e*, quantification of cytoplasmic Ady3 staining. An average of 2–3 areas of ~0.15 μm^2 from each group of 45–50 cells in meiosis II was evaluated using Metamorph software. *Error bars* indicate the standard variation of the brightness measurements. *f*, the width at half-maximum signal intensity of SPB-localized Ady3 signals was measured using line scans preformed orthogonally to the microtubules across the area where Ady3 staining at the ends of microtubules was visible. Metamorph software was used, and ~30–35 cells (2–4 measurements each) per strain were evaluated. *Error bars* represent the S.D. of the measurements. *g*, electron micrographs from representative cells of the strains shown in *panels a–d*. Situations containing an SPB in meiosis II are shown (with the exception of one picture of the Δ*sma1* mutant, where the SPB is not present in the depicted plane). The genotype of the strains is indicated. *nuc.*, nucleus; *NE*, nuclear envelope; *asterisk*, meiotic plaque; *black arrows*, PSMs. *Arrowheads* indicate some vesicles, and *white arrows* points to the inner side of the SPBs.

Interestingly, Ady3p staining at the SPBs was apparent also in the Δ*spo14* and Δ*sma1* mutants, (Fig. 2, *c* and *d*, *white arrowheads*), whereas no rods or donuts indicative of assembled LEP coats and PSMs were seen. For Δ*sma1* few precursor structures remained in the cytoplasm (Fig. 2*d*), whereas in the Δ*spo14* mutant a high staining of Ady3 in the cytoplasm with few discrete precursor structures was seen (Fig. 2*c*; quantification in Fig. 2*e*). Furthermore, the precursor structures seen at the SPBs in the Δ*sma1* mutant appeared larger and brighter than the ones seen in the other mutants (Fig. 2*f*). These data suggest that Spo14 and Sma1 promote prospore membrane assembly at the level of membrane formation at the SPBs during meiosis II, but with recognizable differences between the two mutants.

Using electron microscopy we investigated the precise defect in the Δ*sma1* and Δ*spo14* mutants with regard to the processes of initiation of PSM formation at the SPBs. Once again, we used wild type and Δ*mpc54* Δ*mpc70* mutant strains for comparison (Fig. 2*g*). This comparison revealed that, in the Δ*mpc54* Δ*mpc70* mutant but also in the Δ*spo14* mutant, vesicles of homogeneous size (60–70 nm) could be found adjacent to the cytoplasmic side of the SPBs, whereas in wild type cells an assembled prospore membrane was always visible. In the Δ*spo14* mutant a fully assembled meiotic plaque was visible (Fig. 2*g*), whereas in the Δ*mpc54* Δ*mpc70* mutant this structure was missing as reported previously (14). In the Δ*sma1* mutant the vesicles seemed to have fused to small prospore membranes; however, their enlargement appeared to be impaired, and only small PSMs, often with many vesicles adjacent, were found (Fig. 2*g*). These results suggest that the Δ*spo14* and the Δ*sma1* mutants display different defects during the early process of initiation of prospore membrane biogenesis after the assembly of the meiotic plaque has taken place.

To investigate the localization of Sma1, we tagged the *SMA1* gene on its chromosomal location with GFP. This led to a fully functional gene fusion, as sporulation occurred at wild type frequency in this strain. Western blotting confirmed the expression profiling data showing that Sma1 is only expressed during mid-late phases of meiosis when spore formation is initiated (data not shown) (18). Using immunofluorescence microscopy, we found that Sma1-GFP localizes to the prospore membrane during the stage of membrane growth (Fig. 3*a*). No Sma1-GFP signal was detected in the cells during earlier stages of meiosis when the initiation of prospore membrane assembly has not yet started. Co-immunolabeling of HA-Spo14 and Sma1-GFP in the same cells demonstrated that both proteins localize to the prospore membrane in a similar manner (Fig. 3*b*). Also in the Δ*mpc54* Δ*mpc70* mutants no discrete localization of Sma1-GFP to Ady30-labeled structures was visible (data not shown). In contrast, HA-Spo14p was found to co-localize partially to Ady3-labeled structures in the Δ*mpc54* Δ*mpc70* mutant (Fig. 3*c*), suggesting binding of Spo14 to precursors of the PSM before it becomes

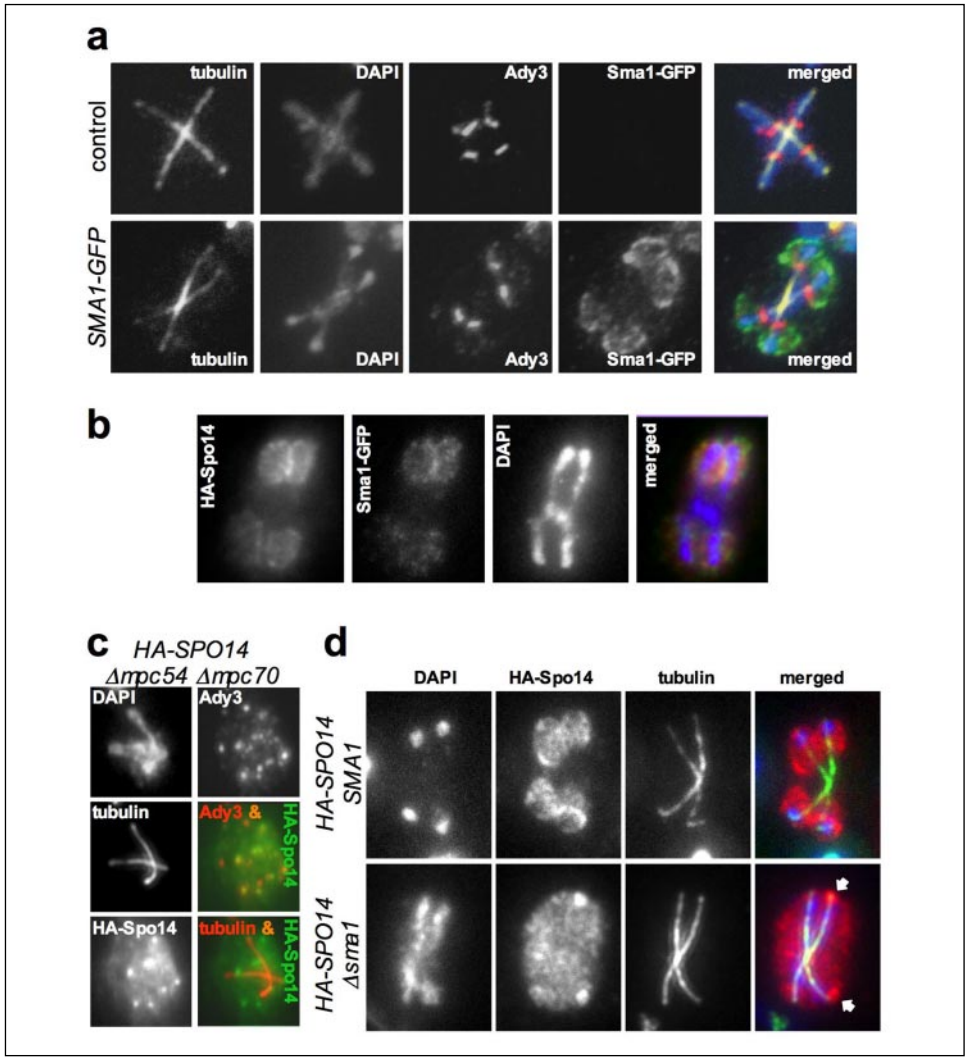

FIGURE 3. **Immunofluorescence localization of Sma1 and Spo14 in meiotic wild type and mutant yeast strains.** *a*, localization of Sma1-GFP to prospore membranes in a representative cell in meiosis II. Antibodies used to detect the specific structures are as indicated. Strain used was YKS233. *b*, co-localization of Sma1-GFP and HA-Spo14 to the prospore membrane of a cell in meiosis II. Strain used was YMM199. *c*, co-localization of HA-Spo14 and Ady3 to precursor structures of the prospore membranes. HA-Spo14 was localized together with Ady3 in the Δ*mpc54* Δ*mpc70* mutant. This mutant is blocked in the assembly of the PSMs because of a defect in the function of the meiotic SPBs (14). One representative cell in meiosis II is shown. *d*, localization of HA-Spo14 in wild type and Δ*sma1* mutant cells to prospore membranes in meiosis II. The strains used were YMK695 and YMK713. *DAPI*, 4,6′-diamidino-2-phenylindole.

assembled. HA-Spo14 localizes all along the prospore membrane, and hardly any HA-Spo14 can be detected in the cytoplasm (Fig. 3*d*, *top row*). In the Δ*sma1* mutant HA-Spo14 could still be found to localize to the small prospore membrane structures that become assembled in this mutant (Fig. 3*d*, *arrows* in *lower row*); however, a cytoplasmic pool of HA-Spo14 was also detected. We could not perform the converse experiment, namely the localization of Sma1 to the prospore membrane in the Δ*spo14* mutant because of the impaired PSM assembly in this strain. Together, these data suggest that Sma1, like Spo14, is a component of the prospore membrane but that Spo14 binding to the prospore membrane is not dependent on Sma1.

We next investigated whether Sma1 is a modulator of Spo14 activity by performing PLD activity measurements in living wild type and Δ*sma1* cells. No difference in the overall phosphatidylcholine (PC)-specific phospholipase D activity was seen when Δ*sma1* cells were compared with wild type cells (Fig. 4*a*). In the Δ*spo14* mutant no activity was found, as reported previously (5). This finding suggests that Sma1 is not required for the enzymatic activity of Spo14 *per se*. To determine whether Sma1 is associated with active PLD/Spo14 in meiotic cells, we performed PLD assays with immunoprecipitated Sma1-HA or HA-Spo14 from meiotic cell extracts. These assays revealed that Sma1 was indeed associated with active PLD (Fig. 4*b*). The activity was similar when Sma1-HA or HA-Spo14 were immunoprecipitated, although

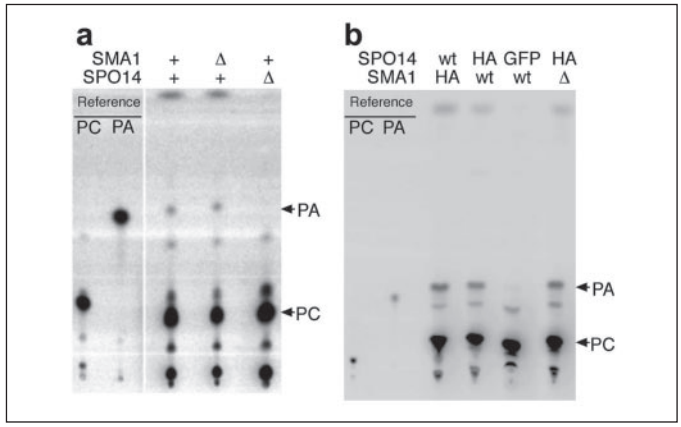

FIGURE 4. **Sma1 is associated with active PLD/Spo14.** *a*, PLD activity assay in cells in meiosis II. Cells with the indicated genotype were incubated with BODIPY-PC (Invitrogen) for 2 h during the stages where the cells undergo meiosis I and meiosis II (4–6 h after induction of meiosis). Total lipids were isolated and separated by thin layer chromatography followed by imaging of BODIPY-fluorescent using a fluorescence scanner. The presence of Spo14 is required for PC conversion to PA in meiotic cells. The strains used were YCR10, YMK691, and YKS53. *b*, PLD activity assay using immunoprecipitated HA-Spo14 and Sma1-HA. Isolated anti-HA immunocomplexes from cells in meiosis II expressing Sma1-HA, HA-Spo14, or GFP-Spo14 (from the same experiment that is shown in Fig. 1*b*) were used for this experiment. Standards were BODIPY-PA and BODIPY-PC (Invitrogen). *wt*, wild type.

Sma1-HA precipitated only a small fraction of Spo14 as compared with the HA-Spo14 precipitations (<2–5%) (Fig. 1*b*). This finding suggests that, whereas only a minor fraction of Spo14 is present in association with Sma1, this fraction is nevertheless highly active.

DISCUSSION

Here we identify Sma1 as the first interaction partner of PLD/Spo14 in budding yeast and examine the role these proteins play during the meiotic cell differentiation processes that lead to the formation of the membranous encapsulation of the spores. The formation of these so-called prospore membranes is entirely different from mitotic bud membrane formation, as these membranes become assembled *de novo* inside the cell, discontinuous to the plasma membrane of the mother cell. Already this topological argument indicates that a specific regulatory mechanism must control PSM biogenesis because it involves the formation of a new acceptor compartment as the starting membrane for the assembly of each PSM. It is known that a structural appendix of the SPB, the meiotic plaque, is essential for the initiation of PSM formation (14). In the absence of a meiotic plaque, vesicular structures have often been found to be associated with the SPBs, apparently unable to initiate membrane formation. However, it is unclear which proteins govern the regulatory mechanisms that ensure the subsequent occurrence of membrane initiation and membrane elongation from the membrane side. Several *sec*-mutants defective for the last step of exocytosis have been shown to be unable to form spores and prospore membranes, which suggests that some steps during the PSM assembly rely on "classical" exocytic machinery (3). In the case of the Δ*spo14* mutant the precise defects were unknown, largely due to the unavailability of cytological markers for PSMs at the time of these studies and the insufficient resolution of the electron microscopic procedures used (5). The study presented here clearly shows that in the Δ*spo14* and the Δ*sma1* mutants the structural appearance of the meiotic plaque is similar to that in the wild type, suggesting that the defect lies in the membrane side of the process. The electron microscopic observation showed an accumulation of vesicles of homogenous size (~60–70 nm) in the Δ*spo14* mutant and of assembled small PSMs in the Δ*sma1* mutant. This shows that different processes are affected in these mutants. The Δ*spo14* mutant phenotype is most consistent with the idea that initiation of PSM formation is dependent on the fusion of vesicles of similar size in order to form an initial acceptor compartment. In contrast, the Δ*sma1* phenotype appears to be due to a defect associated with a process after the initiation of membrane formation, presumably membrane elongation. This observation provides direct genetic evidence that membrane initiation and membrane elongation are distinct processes with different molecular requirements. Recent support for a homotypic vesicle fusion event came from the analysis of the Δ*mso1* mutant, which affects the function of Sec1 and SNARE complex formation in meiosis. In this case, unfused vesicles that are tightly docked to the meiotic plaque are visible (39). The comparison of this phenotype with the one in the Δ*spo14* mutant suggests that the vesicles at the SPBs appear to be much looser bound to the SPBs in the Δ*spo14* mutant. This observation suggests that the vesicle fusion process in the Δ*spo14* mutant is blocked at a slightly earlier step than in the Δ*mso1* mutant.

Spo14 is present in a complex with Sma1 when immunoisolated from meiotic cells but also from mitotic cells. This finding indicates that no meiosis-specific protein is mediating the binding of Sma1 to Spo14 and that this binding is independent of the presence of a prospore membrane. In addition, this result excludes the possibility that the meiosis-specific regulation, which has been previously reported for Spo14 (23), is responsible for the formation of a complex involving these two proteins. Spo14 is a large (195-kDa) protein with several functional domains, among them a pleckstrin homology domain and a catalytic domain (24). We tried a two-hybrid assay to analyze the interaction of Spo14 with Sma1. However, full-length Spo14, as well as several generated subfragments, did not show two-hybrid interaction. This result could either indicate a principal problem associated with the two-hybrid of Sma1 or Spo14 or an additional requirement for an interaction between these proteins. The purification of the Sma1-protein A fusion revealed only Spo14 as a clear interaction partner, whereas the other co-purifying proteins, which were notably present in much smaller amounts, have been described to have functions in completely unrelated processes. These proteins might be contaminations caused by the high charge of Sma1 (pI=10.6). However, we cannot exclude the possibility that among the not yet identified proteins there is an additional factor present in the purified protein complex that is required for the Sma1-Spo14 interaction. Gavin *et al.* (25) reported in their systematic TAP-tagging isolation of yeast protein complexes the co-purification of Spo14 with Mum2. Mum2 is a protein with a presumable function in meiotic prophase (26) and exhibits a similar meiotic expression profile with an expression peak during meiosis II as compared with Sma1 (18). However, using sensitive co-immunoprecipitation and a functional 3×HA-tagged Mum2 construct, which can be detected in mitotic and meiotic cells, we were unable to validate the interaction with Spo14, at least under conditions where Spo14 interacts stably with Sma1 (data not shown).

Spo14 has previously been shown to be essential for Golgi function under circumstances where the deletion of the essential requirement of the phosphatidylinositol transfer protein Sec14 is bypassed by mutations in other genes. The function of Spo14 was thereby genetically linked to the generation of sufficient phosphatidic acid to support Golgi function (27). Using this bypass of Sec14 strain, we addressed the question of whether overexpression of Sma1 would interfere with the function of Spo14. This assay has previously been used to successfully address the function of proteins that interfere with PLD/Spo14 function (28). However, no negative effect of cell growth upon overexpression of Sma1 from a high copy plasmid under control of the strongly inducible Gal1 promoter was seen in this strain. This observation suggests that Sma1 does not negatively interfere with the enzymatic activity or lead to mislocalization of Spo14, as was the case with overexpression of α-synuclein in yeast cells (28). We thus have support for our finding that Spo14 present in the complex with Sma1 is active.[6] It may thus well be that Sma1 plays a role as an activator of Spo14 activity as indicated by the fact that the much lower amounts of Spo14 protein present in the Sma1-HA immunoprecipitates exhibited similar activity as direct HA-Spo14 immunoprecipitates. We have tried to verify the Spo14-activating function of Sma1 directly; however, all our attempts to express functional and soluble Sma1 protein using either *Escherichia coli*, Sf9 cells, or refolding of insoluble Sma1 protein have failed.

The small GTPase Arf1 has been shown to undergo a protein-protein interaction with human PLDs that cause an activation of PLD enzymes (29, 30). Because similar attempts to show a stimulatory function of the yeast Arf1/2 proteins on Spo14 failed (31), however, Sma1 is at present the only protein in yeast shown to interact and potentially stimulate PLD/Spo14 activity.

In higher eukaryotes PLDs have been implicated in various vesicle-related events, especially in vesicle budding from the Golgi and the fusion of secretory vesicles with the plasma membrane, but also in regulation of endocytosis (for a review, see Ref. 32). Effects of PLD function

[6] C. G. Riedel, M. Mazza, P. Maier, R. Körner, and M. Knop, unpublished observations.

on cytoskeletal processes have also been reported (33). In addition, several regulatory activities such as protein kinase C and phospholipids, in particular phosphatidylinositol 4,5-bisphosphate, have been reported to regulate PLDs in mammalian cells and, in part, also in yeast (9, 10, 34). Together, these findings indicate a complex picture of PLD functions. Currently, not much is known about how PLD and its enzymatic activity, namely, the conversion of PC to PA, are linked to the molecular mechanisms of vesicle fusion (35).

It is noteworthy that Spo20 was recently shown to contain an N-terminal peptide sequence that mediates its association with membranes enriched with acidic phospholipids such as PA (36). Spo20 is a target SNARE homologue required for sporulation, and Δ*spo20* mutants are impaired in assembly of spores but not of prospore membranes, although the growth of the prospore membranes appeared to be aberrant and retarded (3, 14). Because PLD/Spo14 hydrolyzes PC to PA, it could be that PLD activity at the SPB and along the PSM allows efficient and specific association of Spo20 to membranes and thus facilitates vesicle fusion with the PSM. Thus, it is possible that Sma1 acts to stimulate Spo14 activity to enable efficient growth of the prospore membrane once its initiation has been achieved.

The detailed molecular dissection of the processes regulating prospore membrane assembly and vesicle fusion at the SPBs will require the reconstitution of the Spo14/Sma1-mediated vesicle fusion processes *in vitro*. Although this will be a challenging task, it should provide detailed insights into the essential molecular events that require the function of PLD/Spo14.

Acknowledgments—We thank A. Moreno-Borchart and K. Strasser for strain constructions.

REFERENCES

1. Nelson, W. J. (2003) *Nature* **422,** 766–774
2. Lynn, R. R., and Magee, P. T. (1970) *J. Cell Biol.* **44,** 688–692
3. Neiman, A. M. (1998) *J. Cell Biol.* **140,** 29–37
4. Jantti, J., Aalto, M. K., Oyen, M., Sundqvist, L., Keranen, S., and Ronne, H. (2002) *J. Cell Sci.* **115,** 409–420
5. Rudge, S. A., Morris, A. J., and Engebrecht, J. (1998) *J. Cell Biol.* **140,** 81–90
6. Huijbregts, R. P., Topalof, L., and Bankaitis, V. A. (2000) *Traffic* **1,** 195–202
7. Liscovitch, M., Czarny, M., Fiucci, G., and Tang, X. (2000) *Biochem. J.* **345,** 401–415
8. Vitale, N., Caumont, A. S., Chasserot-Golaz, S., Du, G., Wu, S., Sciorra, V. A., Morris, A. J., Frohman, M. A., and Bader, M. F. (2001) *EMBO J.* **20,** 2424–2434
9. Sciorra, V. A., Rudge, S. A., Prestwich, G. D., Frohman, M. A., Engebrecht, J., and Morris, A. J. (1999) *EMBO J.* **18,** 5911–5921
10. Sciorra, V. A., Rudge, S. A., Wang, J., McLaughlin, S., Engebrecht, J., and Morris, A. J. (2002) *J. Cell Biol.* **159,** 1039–1049
11. Du, G., Altshuller, Y. M., Vitale, N., Huang, P., Chasserot-Golaz, S., Morris, A. J., Bader, M. F., and Frohman, M. A. (2003) *J. Cell Biol.* **162,** 305–315
12. Rabitsch, K. P., Toth, A., Galova, M., Schleiffer, A., Schaffner, G., Aigner, E., Rupp, C., Penkner, A. M., Moreno-Borchart, A. C., Primig, M., Esposito, R. E., Klein, F., Knop, M., and Nasmyth, K. (2001) *Curr. Biol.* **11,** 1001–1009
13. Guthrie, C., and Fink, G. R. (eds) (1991) *Methods in Enzymology: Guide to Yeast Genetics and Molecular Biology*, Vol. 194, pp. 429 and 663, Academic Press, New York
14. Knop, M., and Strasser, K. (2000) *EMBO J.* **19,** 3657–3667
15. Knop, M., Siegers, K., Pereira, G., Zachariae, W., Winsor, B., Nasmyth, K., and Schiebel, E. (1999) *Yeast* **15,** 963–972
16. Janke, C., Magiera, M. M., Rathfelder, N., Taxis, C., Reber, S., Maekawa, H., Moreno-Borchart, A., Doenges, G., Schwob, E., Schiebel, E., and Knop, M. (2004) *Yeast* **21,** 947–962
17. Moreno-Borchart, A. C., Strasser, K., Finkbeiner, M. G., Shevchenko, A., and Knop, M. (2001) *EMBO J.* **20,** 6946–6957
18. Chu, S., DeRisi, J., Eisen, M., Mulholland, J., Botstein, D., Brown, P. O., and Herskowitz, I. (1998) *Science* **282,** 699–705
19. Moens, P. B., and Rapport, E. (1971) *J. Cell Biol.* **50,** 344–361
20. Okamoto, S., and Iino, T. (1982) *J. Gen. Microbiol.* **128,** 1309–1317
21. Davidow, L. S., Goetsch, L., and Byers, B. (1980) *Genetics* **94,** 581–595
22. Bajgier, B. K., Malzone, M., Nickas, M., and Neiman, A. M. (2001) *Mol. Biol. Cell* **12,** 1611–1621
23. Rudge, S. A., Zhou, C., and Engebrecht, J. (2002) *Genetics* **160,** 1353–1361
24. Exton, J. H. (2002) *Rev. Physiol. Biochem. Pharmacol.* **144,** 1–94
25. Gavin, A. C., Bosche, M., Krause, R., Grandi, P., Marzioch, M., Bauer, A., Schultz, J., Rick, J. M., Michon, A. M., Cruciat, C. M., Remor, M., Hofert, C., Schelder, M., Brajenovic, M., Ruffner, H., Merino, A., Klein, K., Hudak, M., Dickson, D., Rudi, T., Gnau, V., Bauch, A., Bastuck, S., Huhse, B., Leutwein, C., Heurtier, M. A., Copley, R. R., Edelmann, A., Querfurth, E., Rybin, V., Drewes, G., Raida, M., Bouwmeester, T., Bork, P., Seraphin, B., Kuster, B., Neubauer, G., and Superti-Furga, G. (2002) *Nature* **415,** 141–147
26. Davis, L., Barbera, M., McDonnell, A., McIntyre, K., Sternglanz, R., Jin, Q., Loidl, J., and Engebrecht, J. (2001) *Genetics* **157,** 1179–1189
27. Xie, Z., Fang, M., Rivas, M. P., Faulkner, A. J., Sternweis, P. C., Engebrecht, J. A., and Bankaitis, V. A. (1998) *Proc. Natl. Acad. Sci. U. S. A.* **95,** 12346–12351
28. Outeiro, T. F., and Lindquist, S. (2003) *Science* **302,** 1772–1775
29. Brown, H. A., Gutowski, S., Kahn, R. A., and Sternweis, P. C. (1995) *J. Biol. Chem.* **270,** 14935–14943
30. Cockcroft, S., Thomas, G. M., Fensome, A., Geny, B., Cunningham, E., Gout, I., Hiles, I., Totty, N. F., Truong, O., and Hsuan, J. J. (1994) *Science* **263,** 523–526
31. Rudge, S. A., Cavenagh, M. M., Kamath, R., Sciorra, V. A., Morris, A. J., Kahn, R. A., and Engebrecht, J. (1998) *Mol. Biol. Cell* **9,** 2025–2036
32. Exton, J. H. (2002) *FEBS Lett.* **531,** 58–61
33. Zouwail, S., Pettitt, T. R., Dove, S. K., Chibalina, M. V., Powner, D. J., Haynes, L., Wakelam, M. J., and Insall, R. H. (2005) *Biochem. J.* **389,** 207–214
34. Powner, D. J., and Wakelam, M. J. (2002) *FEBS Lett.* **531,** 62–64
35. Ktistakis, N. T., Delon, C., Manifava, M., Wood, E., Ganley, I., and Sugars, J. M. (2003) *Biochem. Soc. Trans.* **31,** 94–97
36. Nakanishi, H., de los Santos, P., and Neiman, A. M. (2004) *Mol. Biol. Cell* **15,** 1802–1815
37. Alani, E., Cao, L., and Kleckner, N. (1987) *Genetics* **116,** 541–545
38. Mumberg, D., Muller, R., and Funk, M. (1995) *Gene* **156,** 119–122
39. Knop, M., Miller, K. J., Mazza, M., Feng, D., Weber, M., Keranen, S., and Jantti, J. (July 19, 2005) *Mol. Biol. Cell* DOI 10.1091/mbc.E05-03-0243